Electronic Supplementary Material (ESI) for ChemComm.

Orbital transitions: insight to energy transfer through an antenna for a organo-lanthanide complex

Waygen Thor[†], Yonghong Zhang[†‡], Ka-Leung Wong[†*], Peter A. Tanner[†*]
[†]Department of Chemistry, Hong Kong Baptist University, Waterloo Road, Kowloon Tong, Hong Kong S.A.R. and [‡]State Key Laboratory of Chemistry and Utilization of Carbon Based Energy Resources, Key Laboratory of Oil and Gas Fine Chemicals, Ministry of Education & Xinjiang Uygur Autonomous Region, Urumqi Key Laboratory of Green Catalysis and Synthesis Technology, College of Chemistry, Xinjiang University, Urumqi 830046, Xinjiang, PR China.

Table of Contents

Part I. Instrumentation

	Title	Page, S
A	**Materials**	3
B	**Syntheses of Complexes**	3
C	**Instruments**	3
D	**Calculations** (Table S1)	3,4

Part II. Results

	Title	Page, S
1	**Optimization**	
Table S2	Normal mode calculations of optimized complexes.	4
Figure S1	The overlaid optimized structures of complexes in gas phase and in solution.	4
2	**Frontier orbitals representations of complexes with different functionals.**	
Figure S2	**Euphen** in gas phase.	5
Table S3	Frontier energy gap of **Euphen** in gas phase.	6
Figure S3	**Euphen** in MeOH.	7
Table S4	Frontier energy gap of **Euphen** in MeOH.	8
Figure S4	**EuTTA** in gas phase.	8
Table S5	Frontier energy gap of **EuTTA** in gas phase.	9
Figure S5	**EuTTA** in MeOH.	9
Table S6	Frontier energy gap of **EuTTA** in MeOH.	10
3	**Frontier orbitals representations of complexes with different basis sets.**	
Figure S6	Comparison of complexes with different basis sets.	10
4	**TDDFT**	
Figure S7	Comparison of experimental and calculated absorption spectra.	11
Figure S8	Selected orbital transitions for **Euphen** in gas phase using PBE0.	11

Table S7	Selected calculated absorption properties for **Euphen** in gas phase using PBE0.	12
Figure S9	Selected orbital transitions for **Euphen** in gas phase using M062X.	12
Table S8	Selected calculated absorption properties for **Euphen** in gas phase using M062X.	12
Figure S10	Selected orbital transitions for **EuTTA** in gas phase using PBE0.	13
Table S9	Selected calculated absorption properties for **EuTTA** in gas phase using PBE0.	13
Figure S11	Selected orbital transitions for **EuTTA** in gas phase using M062X.	14
Table S10	Selected calculated absorption properties for **EuTTA** in gas phase using M062X.	14
Figure S12	Selected orbital transitions for **Euphen** in MeOH using PBE0.	15
Table S11	Selected calculated absorption properties for **Euphen** in MeOH using PBE0.	15
Figure S13	Selected orbital transitions for **Euphen** in MeOH using M062X.	16
Table S12	Selected calculated absorption properties for **Euphen** in MeOH using M062X.	16
Figure S14	Selected orbital transitions for **EuTTA** in MeOH using PBE0.	17
Table S13	Selected calculated absorption properties for **EuTTA** in MeOH using PBE0.	17
Figure S15	Selected orbital transitions for **EuTTA** in MeOH using M062X.	18
Table S14	Selected calculated absorption properties for **EuTTA** in MeOH using M062X.	18
5	**CASSCF/NEVPT2**	
Figure S16	Comparison of experimental and calculated absorption spectra in solution phase.	19
Figure S17	Converged active space of **Euphen** in gas phase.	19
Table S15	Selected calculated absorption properties for **Euphen** in gas phase.	19
Figure S18	Converged active space of **EuTTA** in gas phase.	20
Table S16	Selected calculated absorption properties for **EuTTA** in gas phase.	20
Figure S19	Converged active space of **Euphen** in MeOH.	21
Table S17	Selected calculated absorption properties for **Euphen** in MeOH.	21
Figure S20	Converged active space of **EuTTA** in MeOH.	22
Table S18	Selected calculated absorption properties for **EuTTA** in MeOH.	22

Part I Instrumentation

A. Materials

$EuCl_3.6H_2O$ and $Eu(NO_3)_3.6H_2O$ were purchased from Sigma-Aldrich or TCI (all ≥99.99% trace metals basis) and used without further purification. All organic chemicals were purchased from TCI or Energy Chemical with 98% purity and used without further purification.

B. Syntheses of complexes

Synthesis of $Eu(phen)_2(NO_3)_3$ complexes (Euphen)

The $Eu(phen)_2(NO_3)_3$ samples were synthesized by the literature method.[1] Briefly, a solution of 1,10-phenanthroline (85.9 mg, 2 mmol) in MeCN (50 mL) was added to a solution of $Eu(NO_3)_3$ (1 mmol) in MeCN (25 mL). The mixture was left undisturbed for 1 week; white needle-shaped crystals were obtained. These were filtered, washed several times with MeCN, and dried under vacuum.

$Eu(phen)_2(NO_3)_3$: Yield: 84%; Elemental analysis: found (%): C 40.94; H 2.74; N 14.34. calcd. (%): C 41.28; H 2.31; N 14.04.

Synthesis of $Eu(TTA)_3$phen complexes (EuTTAphen)

The $Eu(TTA)_3$phen samples were synthesized by the literature method.[2] Typically, TTA (3 mmol) and phen (1 mmol) were dissolved in 15 mL ethanol in a flask, with stirring at room temperature. Then, the pH of the solution was adjusted to 7.0 by the addition of NaOH solution (1.0 M). After that, 1 mmol of $EuCl_3$ solution in 5.0 mL of deionized water were then added into the above mixture at 60 ^oC with vigorous stirring for 1.0 h to ensure a complete precipitation. The precipitate was finally filtered, washed repeatedly with ethanol and water, and dried overnight under vacuum.

$Eu(TTA)_3$phen: Yield: 57%; Elemental analysis: found (%): C 46.27; H 2.25; N 2.82. calcd. (%): C 43.43; H 2.02; N 2.81. HRMS (ESI) calcd for $C_{24}H_{12}EuF_9NaO_6S_3^+$ $[Eu(TTA)_3+Na]^+$ 838.8757, found 838.8754. HRMS (ESI) calcd for $C_{25}H_{13}EuF_9NaO_8S_3^+$ $[Eu(TTA)_3+COOH]^-$ 860.8847, found 860.8826.

C. Instruments

The ultraviolet-visible absorption spectra were measured using a thin film in Nujol in the range 200-800 nm by a HP Agilent UV-8453 Spectrophotometer. Solution spectra were measured in 1 cm quartz cuvettes.

D. Calculations

Calculations were performed using Orca version 4.2.1[3, 4] and accessories, together with the use of Avogadro.[5, 6] Various functionals as listed in Table S1 were employed with basis sets such as 6-31+G(d)[7, 8] and def2-TZVP with the Stuttgart in-core effective core potentials[9] and basis sets for the lanthanide ions.[10, 11] In all optimizations the Grimme dispersion correction was used in the calculations.[12, 13] In ORCA, the integration grid was usually set to 6 (Lebedev 590 points) with the final grid 7 (Lebedev 770 points). The nature of the optimized structures were checked with frequency calculations. The cases where repeated optimizations still gave an imaginary frequency is listed in Table S2. The simulated absorption spectra employed the bandwidth of 3000 cm^{-1}.

Complete active space self-consistent field (CASSCF) calculations[14] utilized the natural orbitals from MP2 calculations, which in turn utilized optimized structures. Several trials were

conducted to find the optimum active space. N-Electron Valence State Perturbation Theory (NEVPT2) correction was applied to the CASSCF wavefunctions.[15]
Solvent effects were taken into account by the Conductor-like Polarizable Continuum Model (CPCM) model[16, 17] in ORCA.

Table S1. The percentage of HF exchange in the respective DFT functionals.

DFT Functional	Percentage of HF exchange (%)
B3LYP	20
PBE0	25
PBE	0
M06	27
M062X	54

Part II. Results

Table S2. The optimization of structures of **Euphen** and **EuTTA** as assessed by normal mode calculations.

	Solvation Phase	No. of Imaginary Frequencies	Magnitude of Imaginary Frequency (cm^{-1})
Euphen	Gas phase	0	–
	MeOH	0	–
EuTTA	Gas phase	0	–
	MeOH	1	−18.94

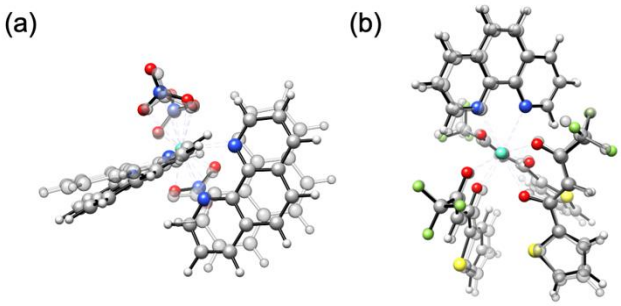

Figure S1. The overlaid optimized structures of (a) **Euphen** and (b) **EuTTA** in MeOH (opaque) with those in the gaseous phase (semi-transparent).

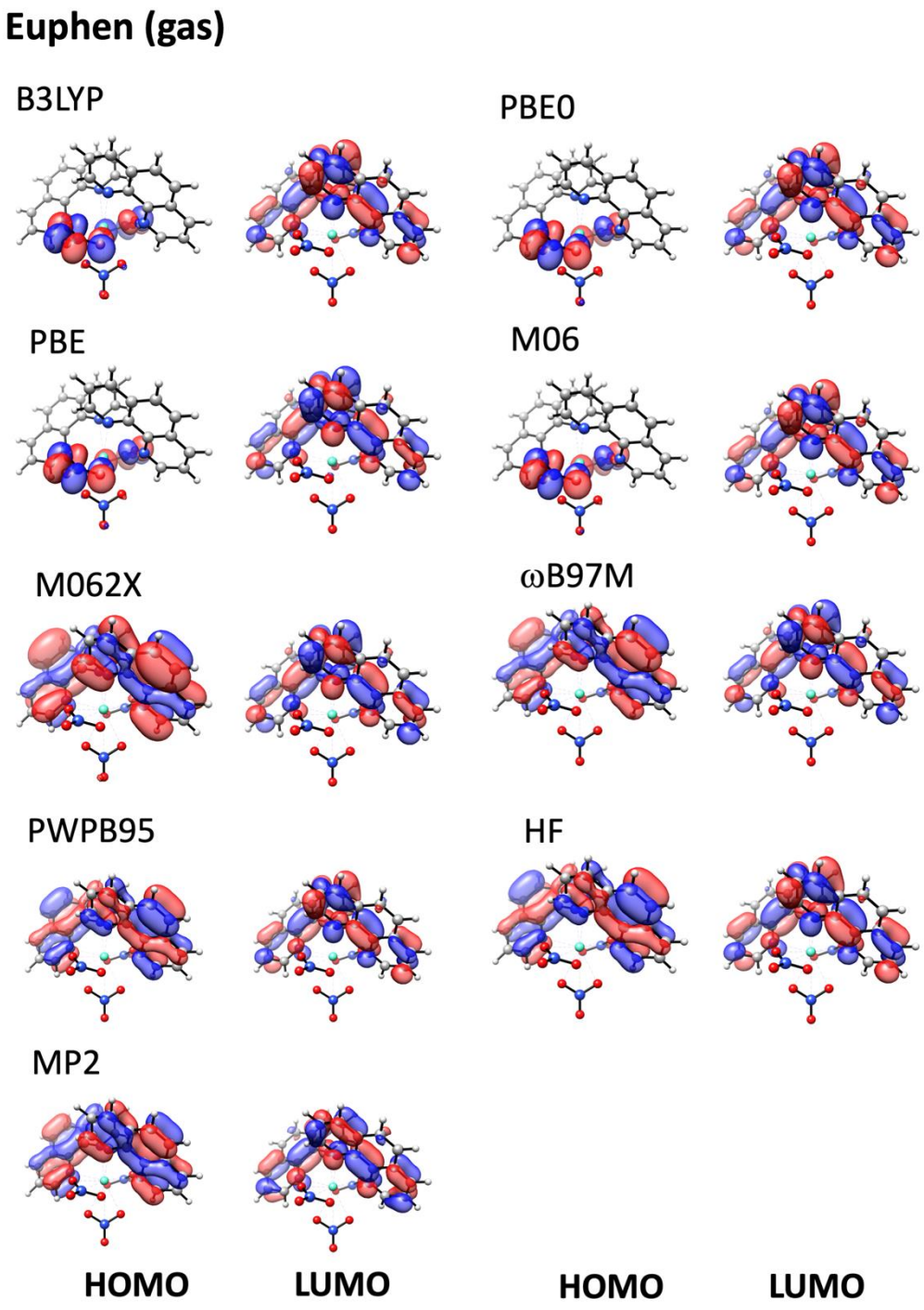

Figure S2. The frontier molecular orbitals of **Euphen** computed in the gas phase using various functionals as indicated.

Table S3. The HOMO, LUMO and the energy gap in eV for **Euphen** computed using different functionals in the gas phase.

Functionals	**HOMO (eV)**	**LUMO (eV)**	**HOMO – LUMO (eV)**
B3LYP	−6.9038	−2.5466	4.3572
PBE0	−7.2556	−2.5033	4.7523
PBE	−5.4587	−3.2728	2.1859
M06	−8.4701	−1.8005	6.6696
M062X	−7.3923	−2.5114	4.8809
WB97M	−9.3757	−0.6449	8.7308
PWPB95	−7.9782	−1.4615	6.5167
HF	−9.0117	0.8789	9.8906
MP2	−8.9576	0.7562	9.7138

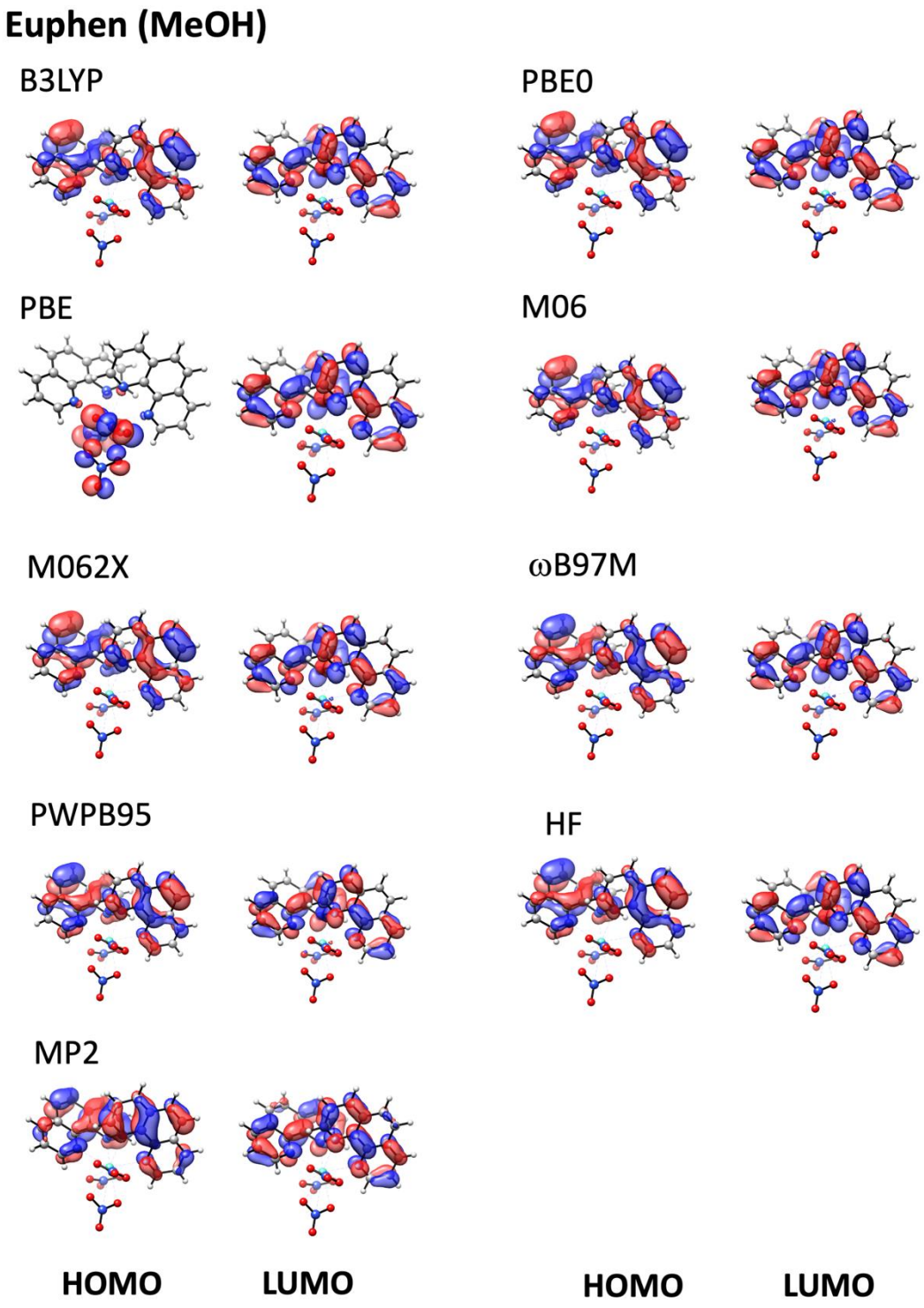

Figure S3. The frontier molecular orbitals of **Euphen** computed in MeOH applying the CPCM method using various functionals as indicated.

Table S4. The HOMO, LUMO and the energy gap in eV for **Euphen** computed using different functionals in MeOH. The band gap is over-estimated in HF and MP2 whereas it is under-estimated for PBE.

Functionals	HOMO (eV)	LUMO (eV)	HOMO – LUMO (eV)
B3LYP	−6.8675	−2.4537	4.4138
PBE0	−7.2167	−2.4505	4.7662
PBE	−6.2438	−3.1919	3.0519
M06	−8.232	−1.7465	6.4855
M062X	−7.2103	−2.4231	4.7872
WB97M	−9.1436	−0.5739	8.5697
PWPB95	−7.7543	−1.4163	6.3380
HF	−8.822	0.9026	9.7246
MP2	−8.7422	0.8325	9.5747

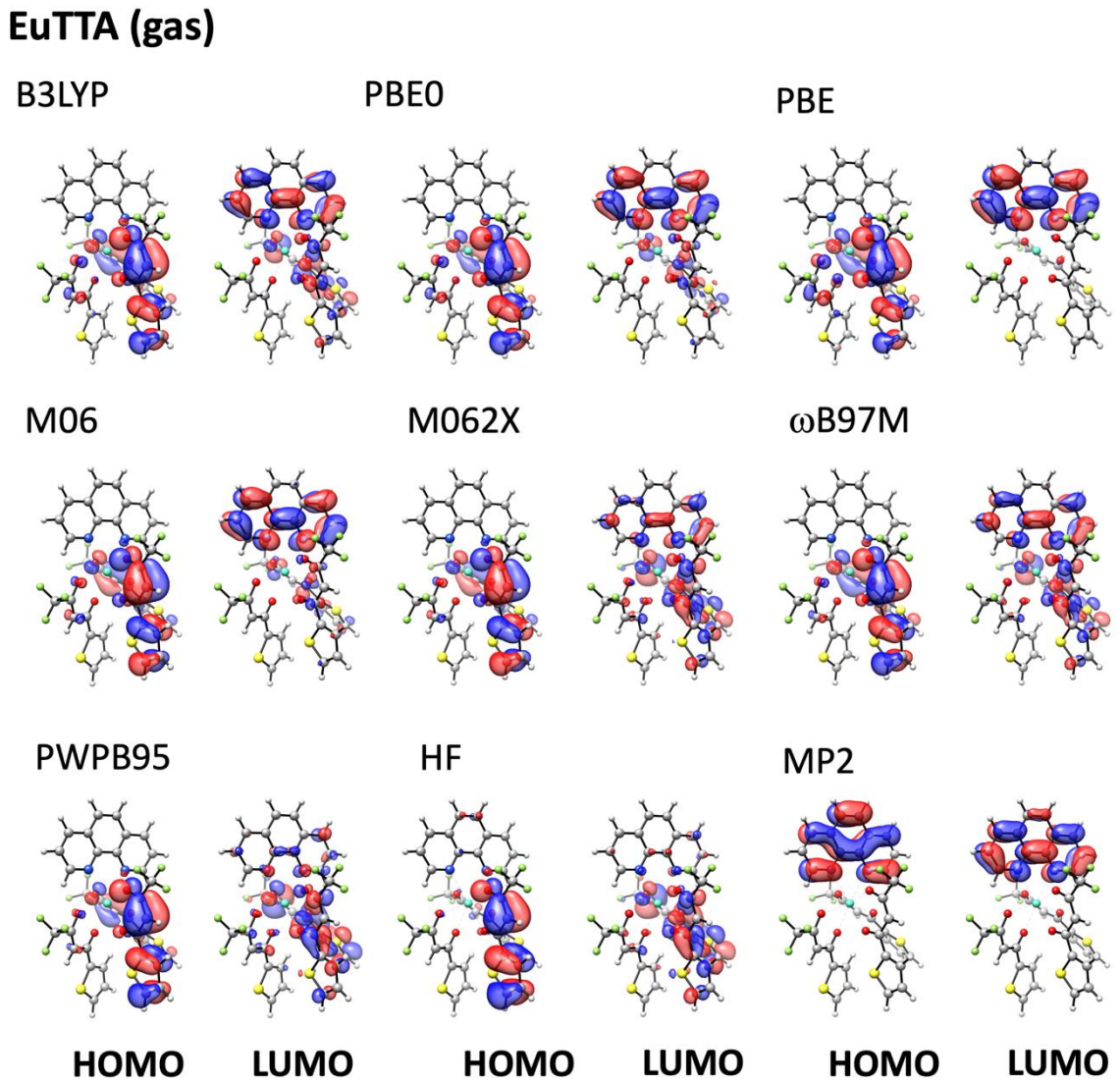

Figure S4. The frontier molecular orbitals of **EuTTA** computed in the gas phase using various functionals as indicated.

Table S5. The HOMO, LUMO and the energy gap in eV for **EuTTA** computed using different functionals in the gas phase.

Functionals	HOMO (eV)	LUMO (eV)	HOMO – LUMO (eV)
B3LYP	−6.1675	−2.2943	3.8732
PBE0	−6.4645	−2.2588	4.2057
PBE	−5.4526	−3.0641	2.3885
M06	−7.5668	−1.5581	6.0087
M062X	−6.5648	−2.2200	4.3448
WB97M	−8.5567	−0.4065	8.1502
PWPB95	−7.1910	−1.2361	5.9549
HF	−8.6515	1.2113	9.8628
MP2	−8.5972	1.0743	9.6715

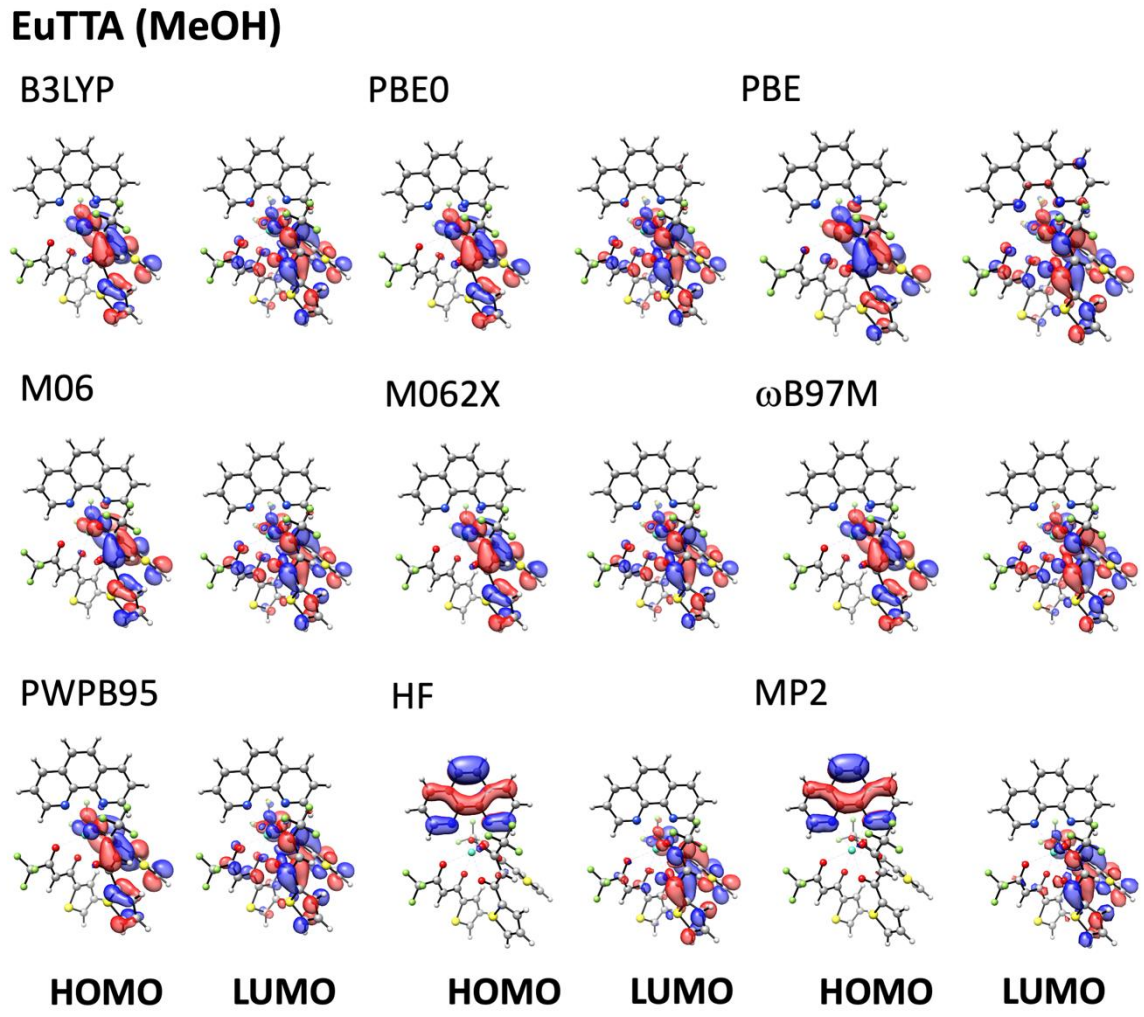

Figure S5. The frontier molecular orbitals of **EuTTA** computed in MeOH applying the CPCM method using various functionals as indicated.

Table S6. The HOMO, LUMO and the energy gap in eV for **EuTTA** computed using different functionals in the MeOH.

Functionals	HOMO (eV)	LUMO (eV)	HOMO – LUMO (eV)
B3LYP	−6.2678	−2.3411	3.9267
PBE0	−6.6101	−2.3276	4.2825
PBE	−5.581	−3.0061	2.5749
M06	−7.7056	−1.6641	6.0415
M062X	−6.7097	−2.2932	4.4165
WB97M	−8.6680	−0.4796	8.1884
PWPB95	−7.3123	−1.3277	5.9846
HF	−8.5602	1.0426	9.6028
MP2	−8.5603	1.0426	9.6029

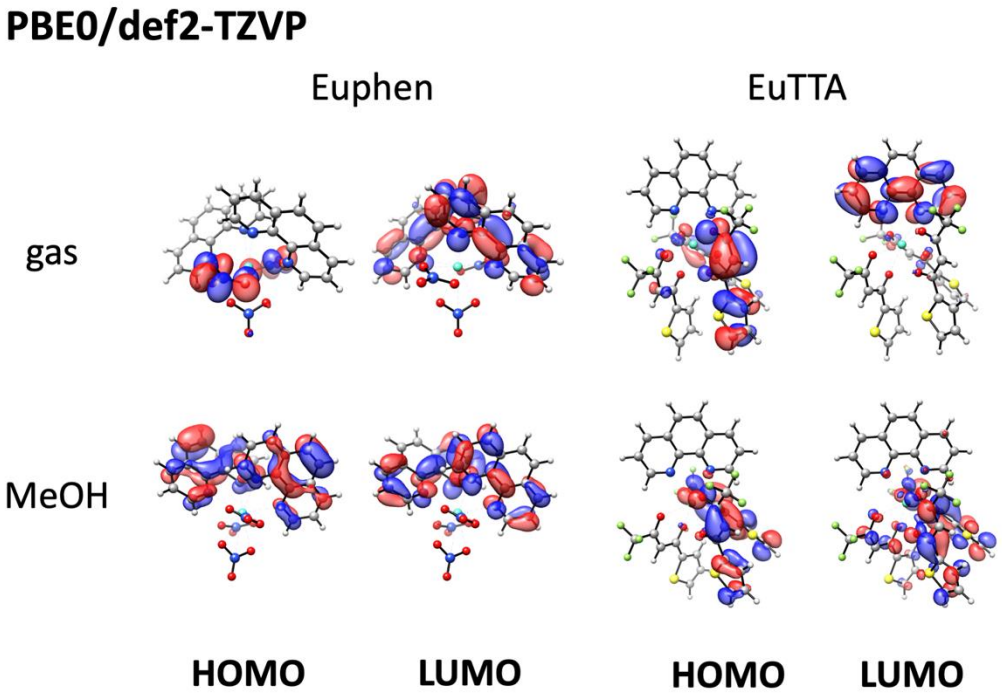

Figure S6. The frontier molecular orbitals of **Euphen** and **EuTTA** computed in the gas phase and MeOH at PBE0-D3BJ/def2-TZVP level of theory. A similar graphical representation of the HOMO and LUMO can be observed as in PBE0-D3ZERO/6-31+G(d).

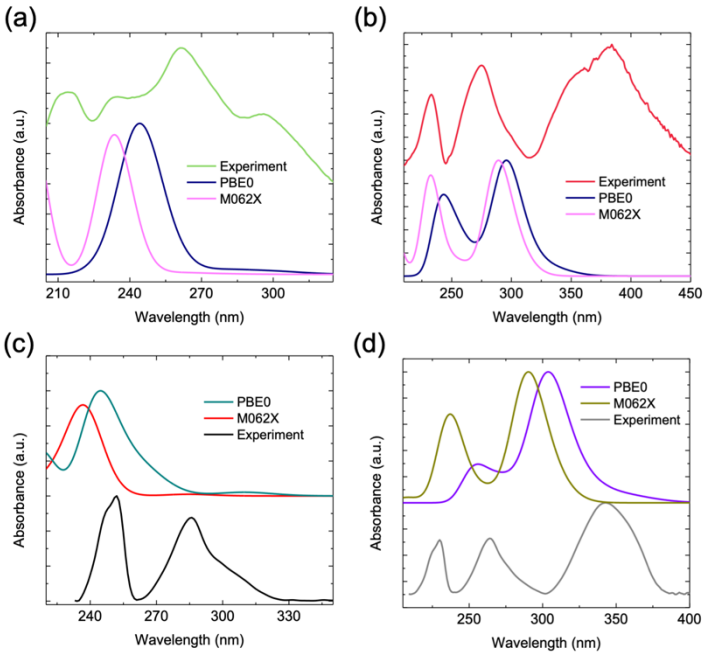

Figure S7. The comparison of experimental absorption spectra of (a) **Euphen** and (b) **EuTTA** to the TD-DFT absorption spectra computed using PBE0 and M062X in the gas phase and (c) **Euphen** and (d) **EuTTA** in MeOH.

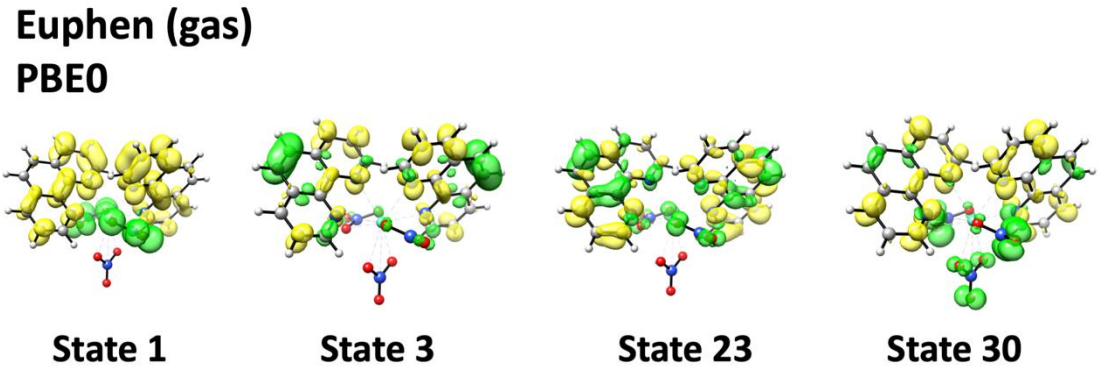

Figure S8. Selected graphical orbital transitions of **Euphen** in gas phase computed using TD-DFT with PBE0-D3BJ/6-31+G(d) level of theory. The green colour indicates a decrease in electron density and yellow indicates an increase.

Table S7. Selected calculated absorption properties with the major composition of **Euphen** in the gas phase from TD-DFT with PBE0-D3BJ/6-31+G(d) level of theory.

State	Wavelength (nm)	Oscillator Strength	Major contribution
1	311	0.00219	HOMO → LUMO (91%)
3	301	0.01209	HOMO – 1 → LUMO (40%)
			HOMO – 2 → LUMO + 1 (19%)
23	264	0.01114	HOMO – 4 → LUMO + 3 (42%)
			HOMO – 1 → LUMO + 2 (26%)
30	252	0.12720	HOMO – 7 → LUMO (30%)

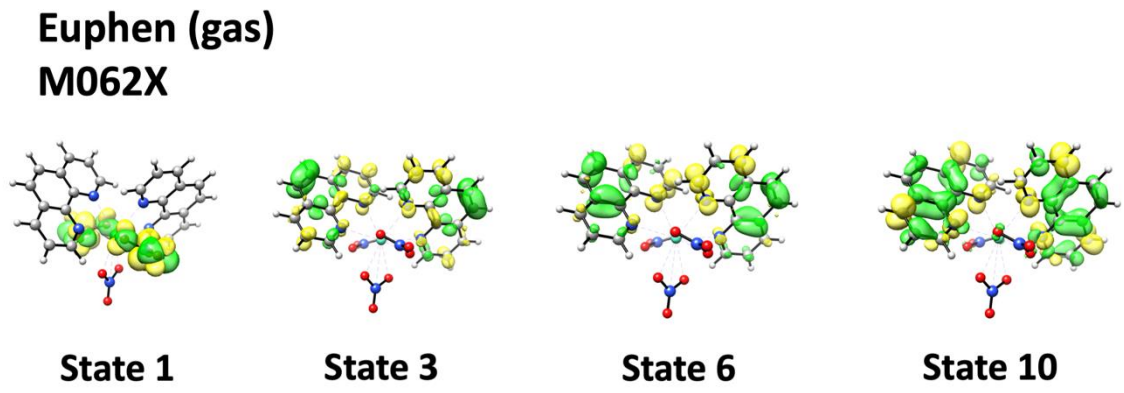

Figure S9. The selected graphical orbital transitions of **Euphen** in the gas phase computed using TD-DFT with M062X-D3ZERO/6-31+G(d) level of theory. The green colour indicates a decrease in electron density and yellow indicates an increase.

Table S8. Selected calculated absorption properties with the major composition of **Euphen** in gas phase from TD-DFT with M062X-D3ZERO/6-31+G(d) level of theory.

State	Wavelength (nm)	Oscillator Strength	Major contribution
1	284	0.00005	HOMO – 6 → LUMO + 15 (35%)
			HOMO – 4 → LUMO + 10 (15%)
			HOMO – 4 → LUMO + 17 (13%)
3	280	0.00400	HOMO → LUMO (37%)
			HOMO – 1 → LUMO + 2 (22%)
6	262	0.01210	HOMO – 1 → LUMO + 2 (26%)
			HOMO – 2 → LUMO (21%)
10	236	0.72235	HOMO – 3 → LUMO (21%)
			HOMO → LUMO + 2 (15%)

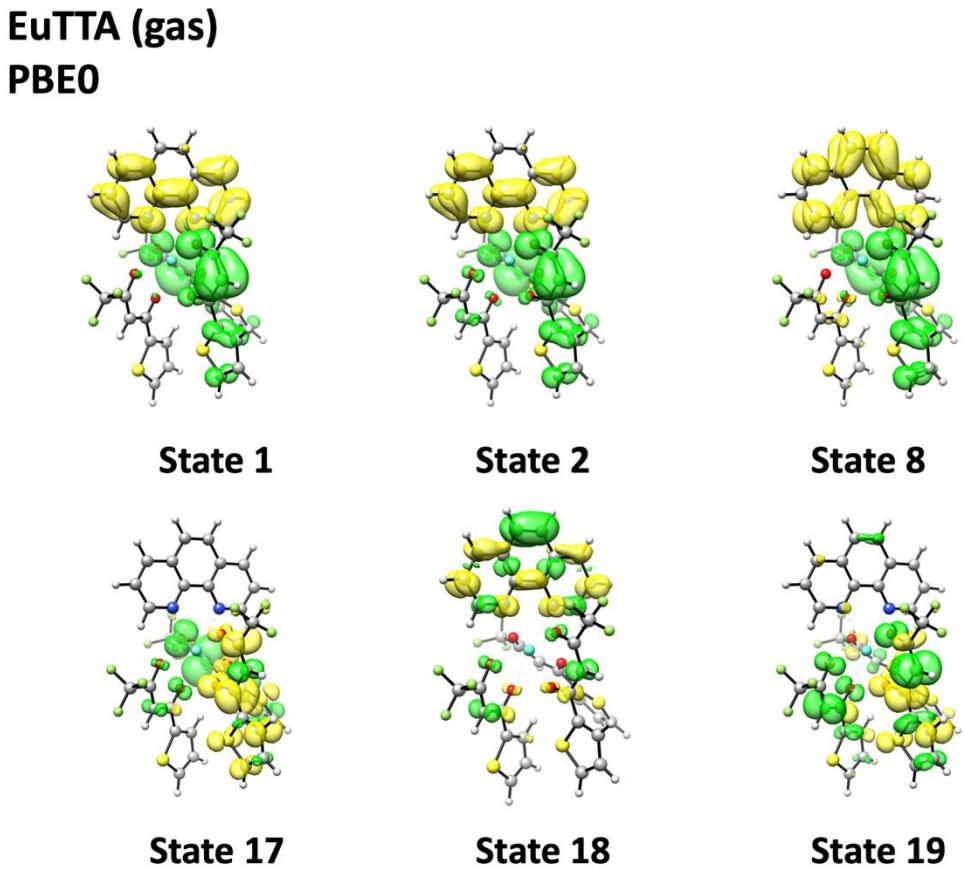

Figure S10. The selected graphical orbital transitions of **EuTTA** in gas phase computed using TD-DFT with PBE0-D3BJ/6-31+G(d) level of theory. The green colour indicates a decrease in electron density and yellow indicates an increase.

Table S9. Selected calculated absorption properties with the major composition of **EuTTA** in gas phase from TD-DFT with PBE0-D3BJ/6-31+G(d) level of theory.

State	Wavelength (nm)	Oscillator Strength	Major contribution
1	347	0.00346	HOMO → LUMO (83%)
2	341	0.03180	HOMO – 1 → LUMO (76%)
8	325	0.01817	HOMO – 1 → LUMO + 2 (50%)
			HOMO → LUMO + 2 (20%)
			HOMO – 1 → LUMO + 1 (15%)
17	305	0.12278	HOMO – 1 → LUMO + 4 (57%)
			HOMO – 1 → LUMO + 3 (15%)
18	298	0.21862	HOMO – 5 → LUMO (48%)
19	294	0.76827	HOMO → LUMO + 4 (28%)
			HOMO – 2 → LUMO + 4 (18%)

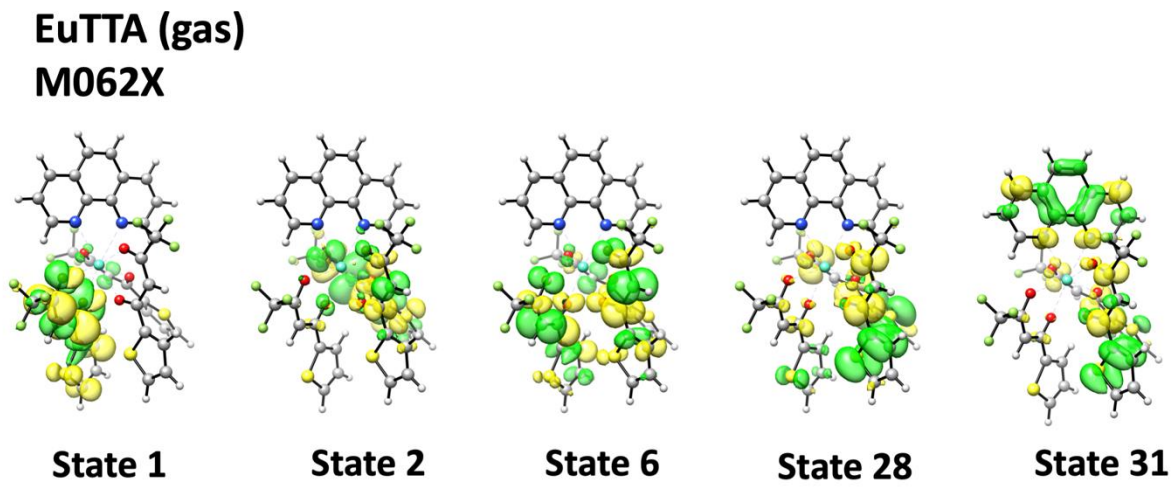

Figure S11. Selected graphical orbital transitions of **EuTTA** in gas phase computed using TD-DFT with M062X-D3ZERO/6-31+G(d) level of theory. The green colour indicates a decrease in electron density and yellow indicates an increase.

Table S10. Selected calculated absorption properties with the major composition of **EuTTA** in gas phase from TD-DFT with M062X-D3ZERO/6-31+G(d) level of theory.

State	Wavelength (nm)	Oscillator Strength	Major contribution
1	309	0.01169	HOMO – 11 → LUMO + 3 (25%)
			HOMO – 12 → LUMO + 3 (19%)
2	305	0.19555	HOMO → LUMO (27%)
			HOMO – 1 → LUMO (24%)
6	288	1.29232	HOMO – 4 → LUMO + 1 (42%)
			HOMO – 9 → LUMO + 2 (25%)
28	237	0.29480	HOMO – 8 → LUMO (26%)
31	232	0.62347	HOMO – 10 → LUMO (11%)
			HOMO – 9 → LUMO + 1 (11%)
			HOMO – 4 → LUMO + 2 (11%)

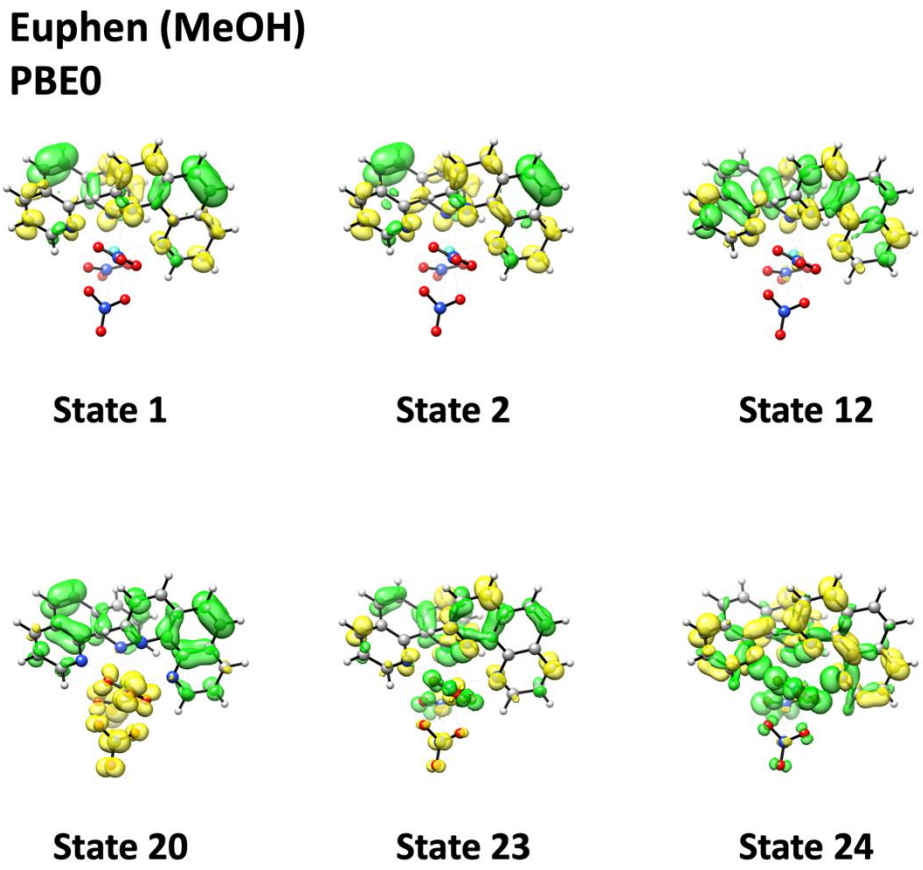

Figure S12. The selected graphical orbital transitions of **Euphen** in MeOH computed using TD-DFT with PBE0-D3BJ/6-31+G(d) level of theory. The green colour indicates a decrease in electron density and yellow indicates an increase.

Table S11. Selected calculated absorption properties with the major composition of **Euphen** in MeOH from TD-DFT with PBE0-D3BJ/6-31+G(d) level of theory.

State	Wavelength (nm)	Oscillator Strength	Major contribution
1	312	0.00875	HOMO → LUMO (78%)
2	310	0.02464	HOMO – 1 → LUMO (74%)
12	268	0.09147	HOMO – 3 → LUMO + 1 (39%)
			HOMO – 2 → LUMO (35%)
20	255	0.10695	HOMO – 1 → LUMO + 4 (39%)
			HOMO – 3 → LUMO + 2 (18%)
23	243	0.40685	HOMO – 7 → LUMO (16%)
			HOMO – 3 → LUMO + 1 (15%)
24	244	0.15873	HOMO – 7 → LUMO (38%)
			HOMO – 5 → LUMO (18%)

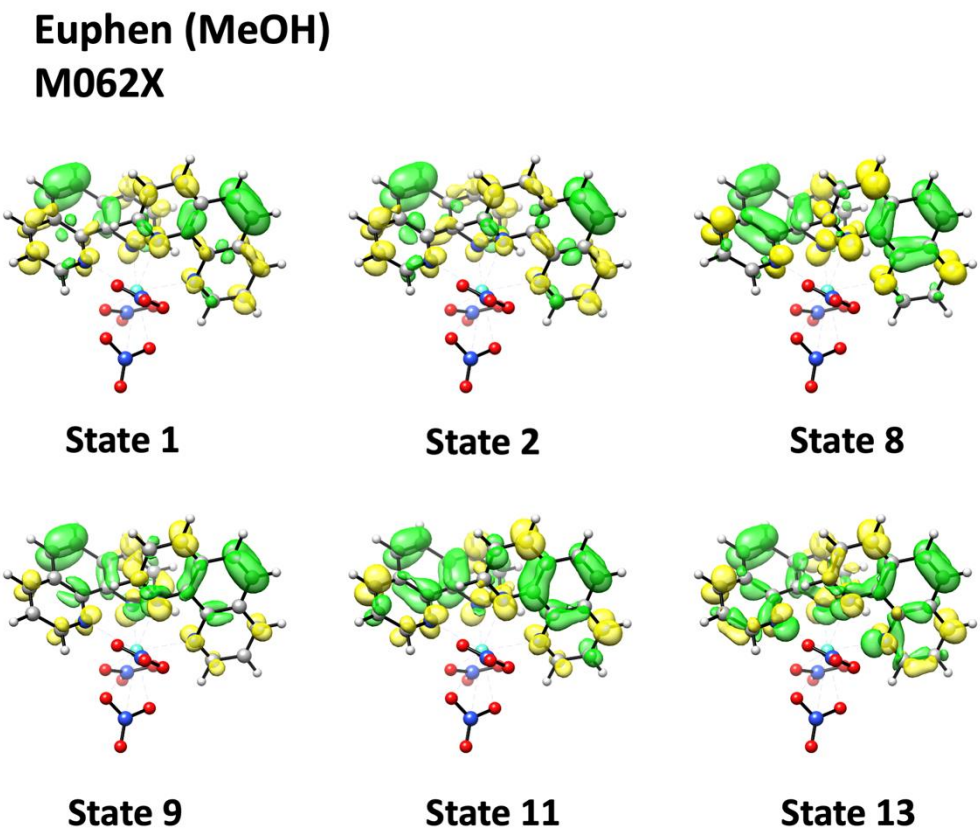

Figure S13. The selected graphical orbital transitions of **Euphen** in MeOH computed using TD-DFT with M062X-D3ZERO/6-31+G(d) level of theory. The green colour indicates a decrease in electron density and yellow indicates an increase.

Table S12. Selected calculated absorption properties with the major composition of **Euphen** in MeOH from TD-DFT with M062X-D3ZERO/6-31+G(d) level of theory.

State	Wavelength (nm)	Oscillator Strength	Major contribution
1	286	0.00548	HOMO → LUMO (49%)
			HOMO − 1 → LUMO + 1 (23%)
2	284	0.01672	HOMO − 1 → LUMO (43%)
			HOMO → LUMO + 1 (26%)
8	243	0.22826	HOMO → LUMO (22%)
			HOMO − 1 → LUMO + 1 (21%)
9	240	0.11777	HOMO − 1 → LUMO (42%)
11	237	0.76593	HOMO − 2 → LUMO (38%)
			HOMO → LUMO + 1 (17%)
13	230	0.10086	HOMO → LUMO + 1 (20%)
			HOMO → LUMO + 3 (20%)

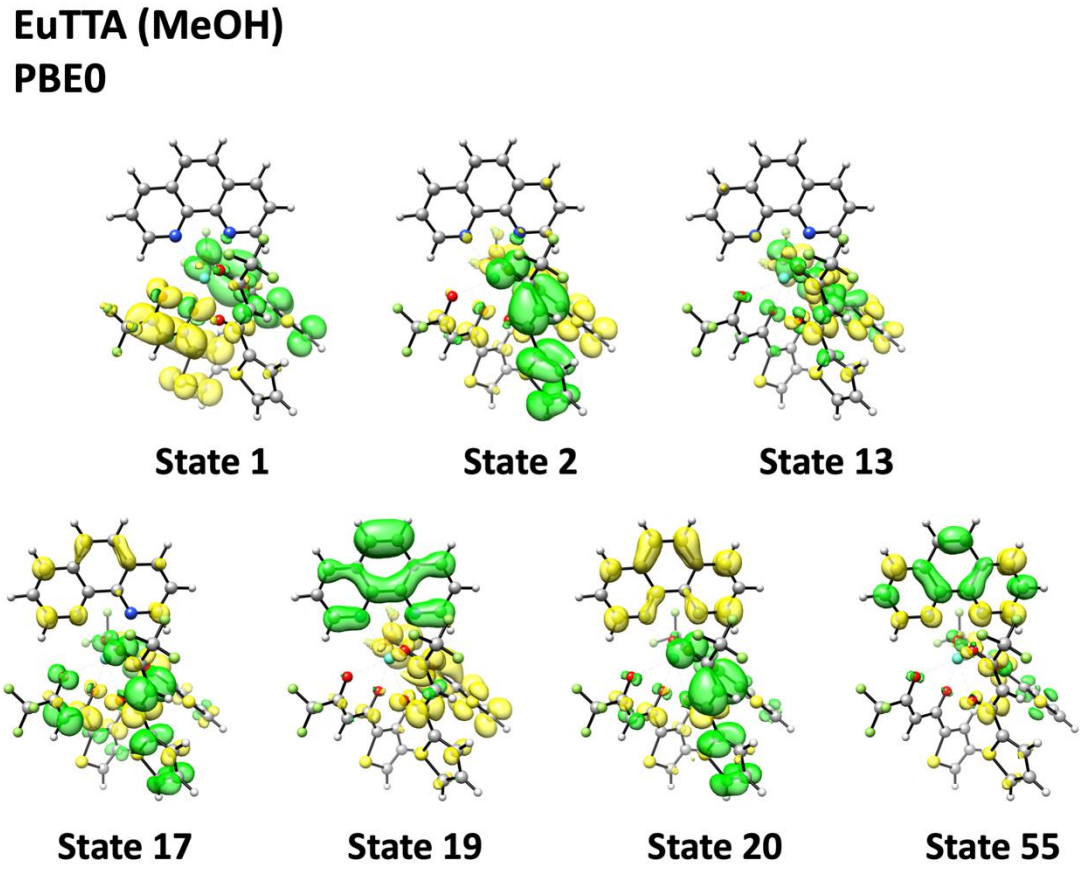

Figure S14. Selected graphical orbital transitions of **EuTTA** in MeOH computed using TD-DFT with PBE0-D3BJ/6-31+G(d) level of theory. The green colour indicates a decrease in electron density and yellow indicates an increase.

Table S13. Selected calculated absorption properties with the major composition of **EuTTA** in MeOH from TD-DFT with PBE0-D3BJ/6-31+G(d) level of theory.

State	Wavelength (nm)	Oscillator Strength	Major contribution
1	374	0.00857	HOMO → LUMO (41%)
			HOMO → LUMO + 1 (38%)
2	358	0.01759	HOMO − 1 → LUMO (37%)
			HOMO → LUMO (34%)
13	308	0.10109	HOMO − 13 → LUMO (15%)
			HOMO − 1 → LUMO + 2 (11%)
			HOMO − 1 → LUMO + 3 (10%)
17	300	0.57422	HOMO − 1 → LUMO + 4 (16%)
			HOMO − 2 → LUMO + 1 (13%)
19	327	0.10685	HOMO − 3 → LUMO + 1 (72%)
20	303	0.27895	HOMO − 1 → LUMO + 4 (47%)
55	253	0.12271	HOMO − 8 → LUMO + 4 (25%)
			HOMO − 3 → LUMO + 5 (16%)
			HOMO − 7 → LUMO + 4 (13%)

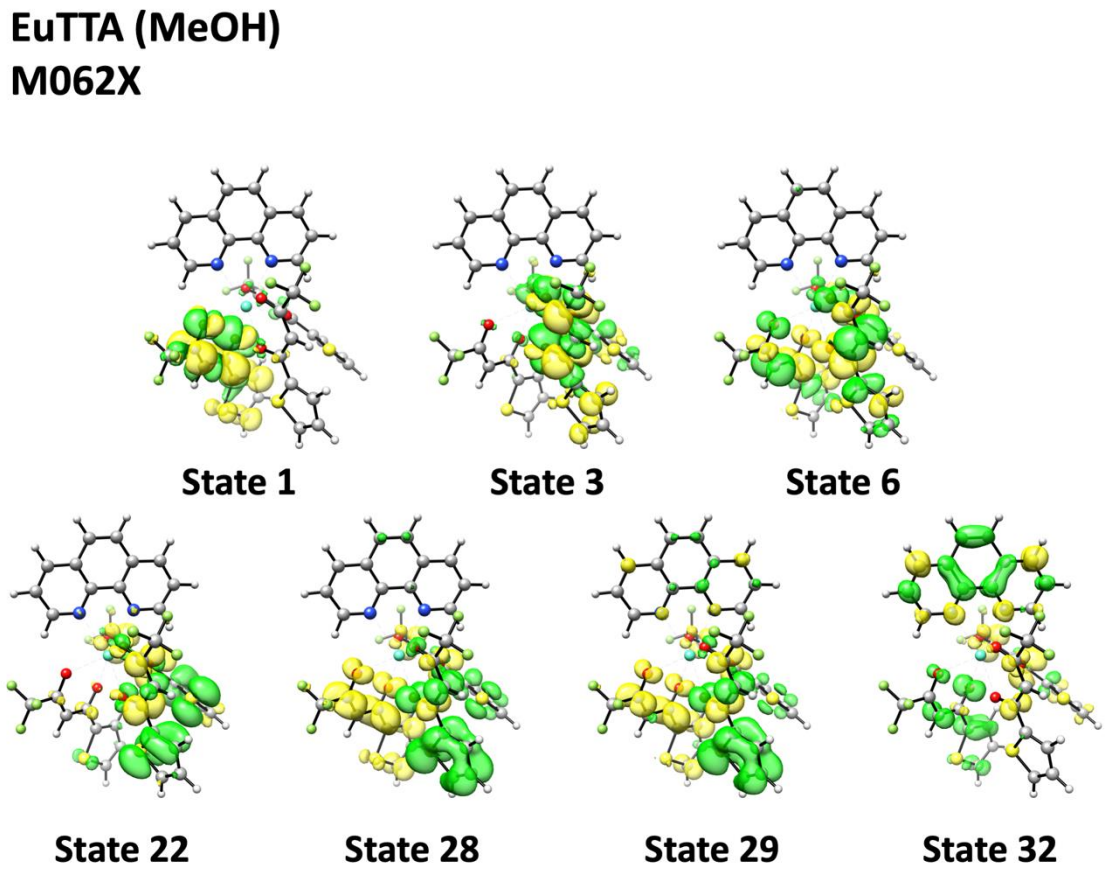

Figure S15. Selected graphical orbital transitions of **EuTTA** in MeOH computed using TD-DFT with M062X-D3ZERO/6-31+G(d) level of theory. The green colour indicates a decrease in electron density and yellow indicates an increase.

Table S14. Selected calculated absorption properties with the major composition of **EuTTA** in MeOH from TD-DFT with M062X-D3ZERO/6-31+G(d) level of theory.

State	Wavelength (nm)	Oscillator Strength	Major contribution
1	312	0.00806	HOMO – 12 → LUMO + 1 (25%)
			HOMO − 11 → LUMO + 1 (19%)
3	306	0.14216	HOMO → LUMO (24%)
			HOMO − 11→ LUMO (14%)
6	289	1.36629	HOMO − 1 → LUMO (34%)
			HOMO − 2 → LUMO + 1 (23%)
			HOMO → LUMO + 2 (12%)
22	245	0.18150	HOMO − 9 → LUMO (24%)
			HOMO − 8 → LUMO (15%)
28	241	0.14163	HOMO − 4 → LUMO + 1 (26%)
29	237	0.18314	HOMO – 4 → LUMO + 1 (27%)
32	233	0.31221	HOMO − 7 → LUMO (12%)

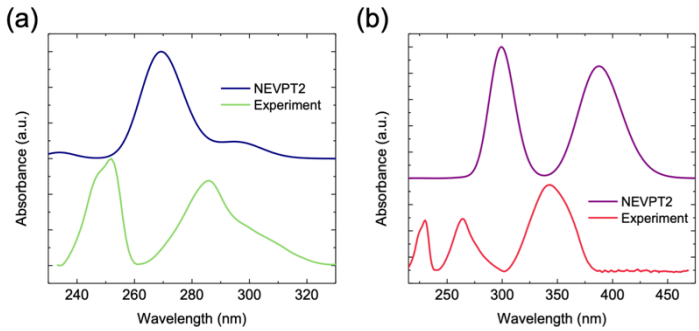

Figure S16. The comparison of experimental absorption spectra of (a) **Euphen** and (b) **EuTTA** to the CASSCF/NEVPT2 (4,5) absorption spectra in MeOH.

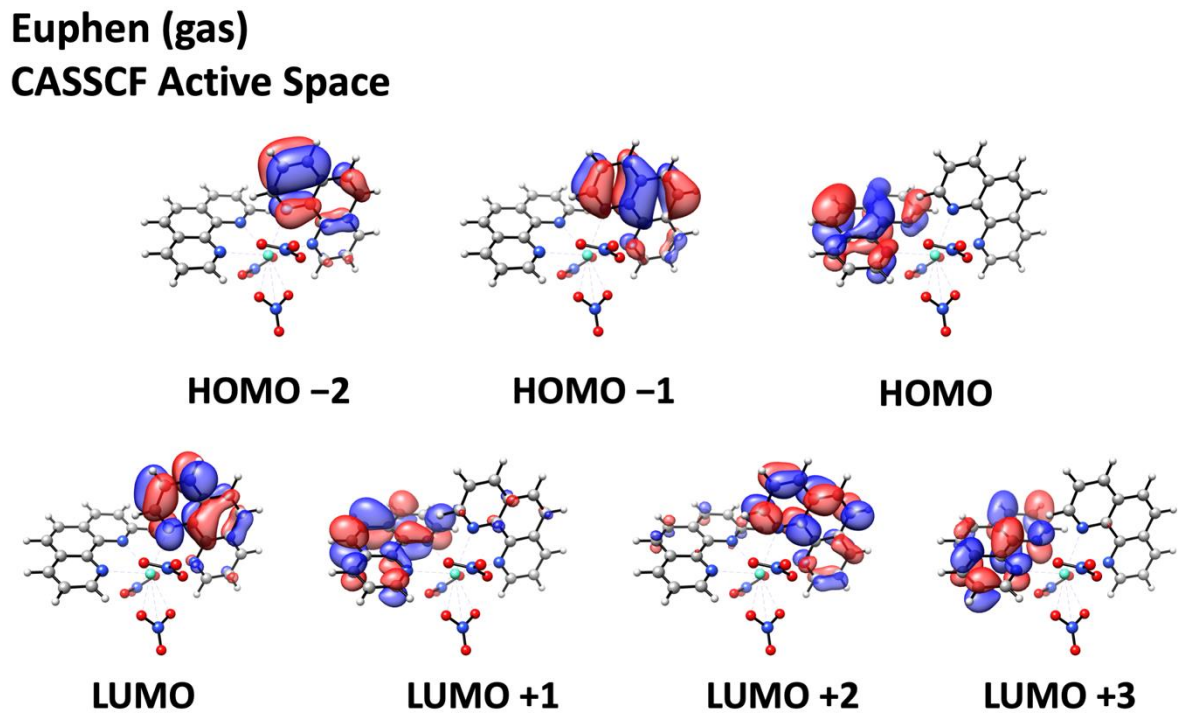

Figure S17. The active space of **Euphen** in gas phase computed using CASSCF level of theory after convergence.

Table S15. Selected calculated absorption properties with the major composition of **Euphen** in gas phase CASSCF with NEVPT2 corrections.

State	Wavelength (nm)	Oscillator Strength	Major contribution
2	297	0.31462	HOMO → LUMO + 3 (81%)
3	263	0.92075	HOMO → LUMO + 1 (77%)
6	217	1.13159	HOMO – 2 → LUMO (32%)
			HOMO – 2 → LUMO + 2 (28%)
			HOMO – 1 → LUMO (14%)
9	216	0.56198	HOMO – 2 → LUMO (25%)
			HOMO – 1 → LUMO +2 (23%)
			HOMO – 1→ LUMO (12%)
			HOMO – 1→ LUMO +2 (11%)

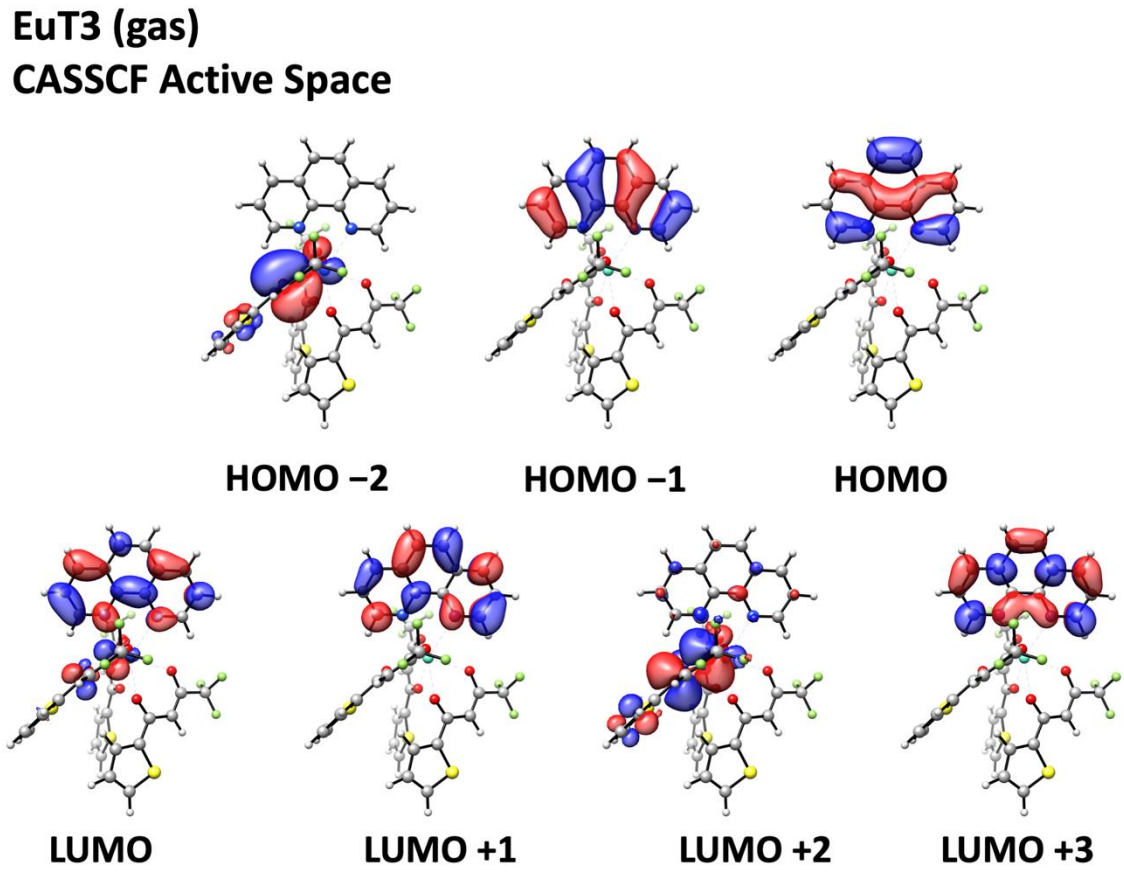

Figure S18. The active space of **EuTTA** in gas phase computed using CASSCF level of theory after convergence.

Table S16. Selected calculated absorption properties with the major composition of **EuTTA** in gas phase CASSCF with NEVPT2 corrections.

State	Wavelength (nm)	Oscillator Strength	Major contribution
1	393	0.25121	HOMO – 2 → LUMO + 2 (74%)
2	255	1.28214	HOMO – 1 → LUMO + 1 (20%)
			HOMO – 1 → LUMO (17%)
			HOMO → LUMO + 1 (14%)
			HOMO → LUMO (14%)
			HOMO – 1 → LUMO + 3 (12%)
3	218	0.96508	HOMO → LUMO + 3 (44%)
			HOMO – 1 → LUMO + 1 (24%)
4	204	0.47910	HOMO – 1 → LUMO + 3 (71%)

Euphen (MeOH)
CASSCF Active Space

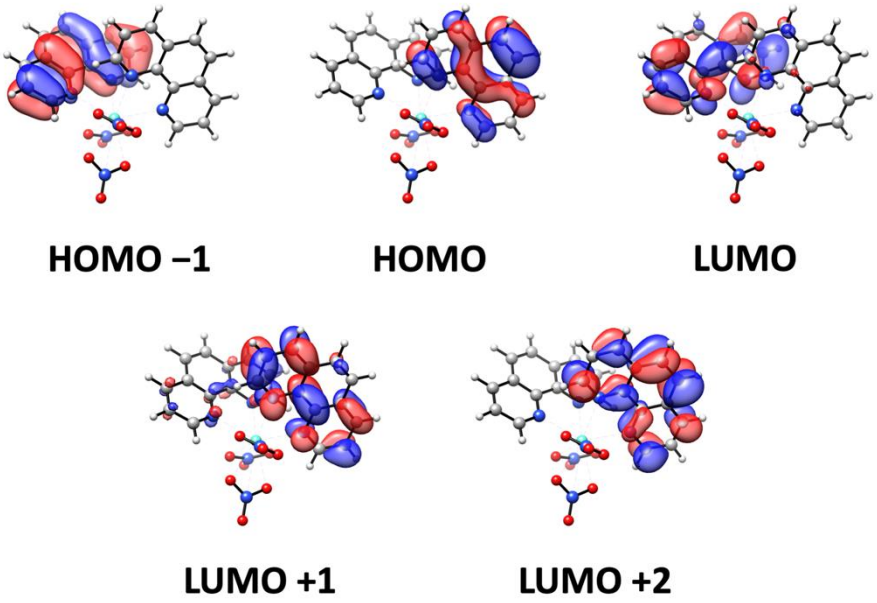

Figure S19. The active space of **Euphen** in MeOH computed using CASSCF level of theory after convergence.

Table S17. Selected calculated absorption properties with the major composition of **Euphen** in MeOH CASSCF with NEVPT2 corrections.

State	Wavelength (nm)	Oscillator Strength	Major contribution
1	313	0.24167	HOMO → LUMO + 1 (79%)
			HOMO → LUMO (17%)
2	282	0.40700	HOMO – 1→ LUMO (82%)
3	272	1.32589	HOMO → LUMO + 2 (82%)
5	226	0.07288	HOMO – 1 → LUMO + 1 (96%)

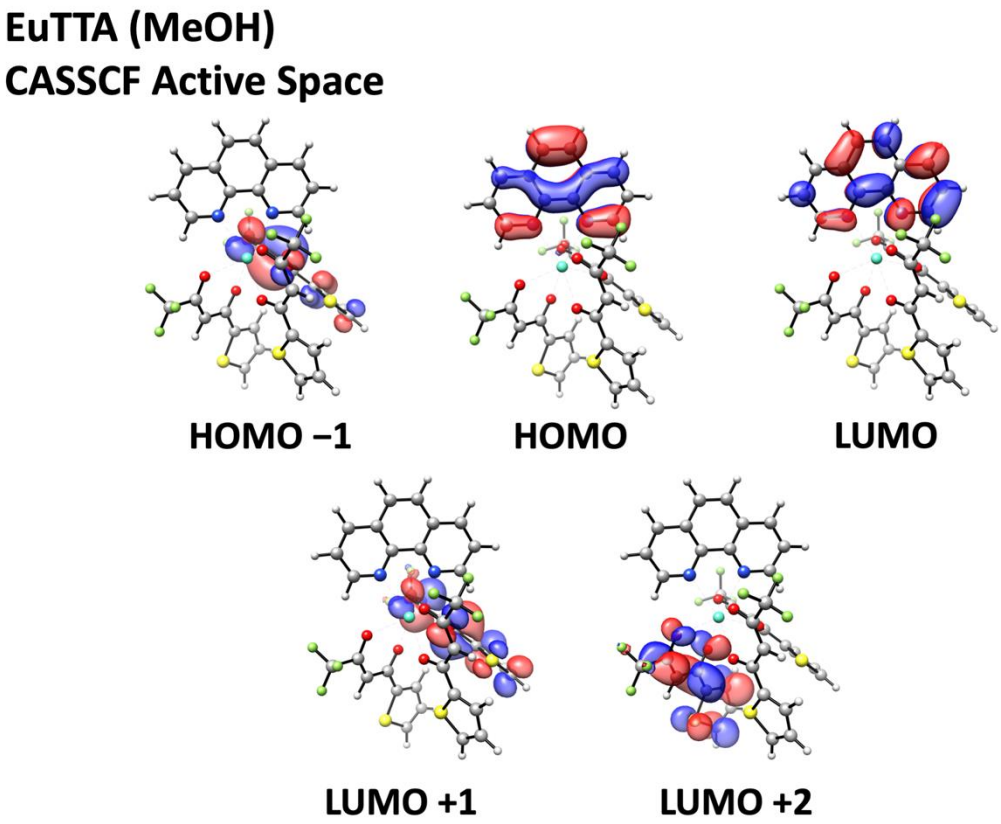

Figure S20. The active space of **EuTTA** in MeOH computed using CASSCF level of theory after convergence.

Table S18. Selected calculated absorption properties with the major composition of **EuTTA** in MeOH CASSCF with NEVPT2 corrections.

State	Wavelength (nm)	Oscillator Strength	Major contribution
1	388	0.44632	HOMO – 1 → LUMO + 1 (93%)
3	299	0.52275	HOMO → LUMO (97%)
5	267	0.00381	HOMO – 1 → LUMO (80%)
11	179	0.00971	HOMO – 1 → LUMO (74%)

References

1. Z. Pan, G. Jia, C.-K. Duan, W.-Y. Wong, W.-T. Wong and P. A. Tanner, *European Journal of Inorganic Chemistry*, 2011, **2011**, 637-646.
2. M. Meng, M. Bai, Z. Da, Y. Cui, B. Li and J. Pan, *Journal of Luminescence*, 2019, **208**, 24-32.
3. F. Neese, *WIREs Computational Molecular Science*, 2012, **2**, 73-78.
4. F. Neese, *WIREs Computational Molecular Science*, 2018, **8**, e1327.
5. M. D. Hanwell, D. E. Curtis, D. C. Lonie, T. Vandermeersch, E. Zurek and G. R. Hutchison, *Journal of Cheminformatics*, 2012, **4**, 17.
6. Avogadro: an open-source molecular builder and visualization tool. Version 1.2.0. http://avogadro.cc/
7. R. Ditchfield, W. J. Hehre and J. A. Pople, *The Journal of Chemical Physics*, 1971, **54**, 724-728.
8. W. J. Hehre, R. Ditchfield and J. A. Pople, *The Journal of Chemical Physics*, 1972, **56**, 2257-2261.
9. Energy-consistent Pseudopotentials of the Stuttgart/Cologne Group, available at: http://www.tc.uni-koeln.de/PP/clickpse.en.html.
10. M. Dolg, H. Stoll, A. Savin and H. Preuss, *Theoretica chimica acta*, 1989, **75**, 173-194.
11. D. Andrae, U. Häußermann, M. Dolg, H. Stoll and H. Preuß, *Theoretica chimica acta*, 1990, **77**, 123-141.
12. S. Grimme, J. Antony, S. Ehrlich and H. Krieg, *The Journal of Chemical Physics*, 2010, **132**, 154104.
13. S. Grimme, S. Ehrlich and L. Goerigk, *Journal of Computational Chemistry*, 2011, **32**, 1456-1465.
14. D. Aravena, M. Atanasov and F. Neese, *Inorganic Chemistry*, 2016, **55**, 4457-4469.
15. C. Angeli, R. Cimiraglia, S. Evangelisti, T. Leininger and J. P. Malrieu, *The Journal of Chemical Physics*, 2001, **114**, 10252-10264.
16. J. Tomasi, B. Mennucci and R. Cammi, *Chemical Reviews*, 2005, **105**, 2999-3094.
17. V. Barone and M. Cossi, *The Journal of Physical Chemistry A*, 1998, **102**, 1995-2001.